

 Open access • Proceedings Article • DOI:10.1117/12.600630

High-RI resist polymers for 193 nm immersion lithography — [Source link](#)

[Andrew K. Whittaker](#), [Idriss Blakey](#), [Heping Liu](#), [David J. Hill](#) ...+3 more authors

Institutions: [University of Queensland](#), [Queensland University of Technology](#), [SEMATECH](#)

Published on: 04 May 2005

Topics: [Immersion lithography](#), [Resist](#), [Photolithography](#), [High-refractive-index polymer](#) and [Plasma etching](#)

Related papers:

- [Nanocomposite liquids for 193 nm immersion lithography: a progress report](#)
- [Novel high-index resists for 193-nm immersion lithography and beyond](#)
- [High Index Resists for 193 nm Immersion Lithography](#)
- [High-index nanocomposite photoresist for 193-nm lithography](#)
- [High Index Resist for 193 nm Immersion Lithography](#)

Share this paper:    

View more about this paper here: <https://typeset.io/papers/high-ri-resist-polymers-for-193-nm-immersion-lithography-4ukhx9olcm>

High-RI Resist Polymers for 193 nm Immersion Lithography

Andrew K. Whittaker^{*a}, Idriss Blakey^a, Heping Liu^a, David J. T. Hill^d, Graeme A. George^c, Will Conley^b and Paul Zimmerman^b.

^aCentre for Magnetic Resonance, Univ. of Queensland, St. Lucia, Qld, 4072, Australia.

^bSEMATECH, 2706 Montopolis Drive. Austin TX, USA 78741.

^cQueensland Univ. of Technology, Brisbane Qld, 4001, Australia

^dSchool of Molecular and Microbial Sciences, Univ. of Queensland, St. Lucia, Qld, 4072, Australia.

ABSTRACT

A critical aim within the field of 193 nm immersion lithography is the development of high refractive index immersion fluids and resists. Increases in the refractive index (RI) of the immersion fluid will result in increases in the numerical aperture and depth of focus. Increasing the RI of resist polymers will improve exposure latitude for the process. A challenge for increasing the RI of resist polymers is to do so without detrimentally affecting other properties of the polymer such as transparency, line edge roughness, adhesion and plasma etch resistance. It is well known in the literature that introducing sulfur, bromine or aromatic groups into a polymer structure will increase its RI. However, due to the relatively strong absorption of phenyl groups at 193 nm these groups have to be avoided. Furthermore, the use of bromine poses problems associated with contamination of the silicon wafer. Hence, in this study, a systematic approach has been used to increase the sulfur content of 193 nm type resist polymers, by synthesis of sulfur-containing monomers and by performing bulk modifications of the polymer. The effect of sulfur content on the RI at 193 nm was then investigated. A broad study of the relationship between molecular structure and RI dispersion from 250-180 nm has also been undertaken, and conclusions drawn using QSPR methodologies. Finally, the effect of sulfur content on other lithography parameters, such as transparency, adhesion and plasma etch resistance, was also evaluated.

Keywords: Immersion Lithography, Resist polymers, high RI, RI dispersion, sulfur, QSPR

1. INTRODUCTION

Immersion photolithography at 193 nm is expected to be utilized for integrated circuit manufacture at the 65 nm and 45 nm nodes. Advances in immersion fluid and resist design could extend 193 nm immersion lithography down to the 35 nm or possibly the 22 nm nodes. An increase in the refractive index (RI) of the immersion fluid has the effect of increasing the NA of a system, (see Eq. (1)), which in turn reduces the possible feature size. Increasing the RI of the fluid also increases the depth of focus (DOF). Similarly, an increase in the RI of the resist also results in improved DOF. For example, in the case of a fluid with an RI of 1.63, changing the RI of the polymer from 1.7 to 1.93 results in an increase in exposure latitude of about 13%.¹

$$R = k_1 \frac{\lambda}{NA} \text{ where } NA = n \cdot \sin \Theta_0 \quad (1)$$

- R = feature size
- λ = wavelength
- NA = numerical aperture
- n = refractive index
- $\sin \Theta_0$ = incident angle

An example of a typical 'dry' 193nm resist polymer is depicted in Fig. 1.² Such polymers have a RI of about 1.7 at 193 nm.³ Apart from this, there is little information published on the refractive index of organic molecules or polymers at 193 nm.

The aims of our study have been to identify new high refractive index polymers that may be utilized as resist polymers. The development of novel polymers using conventional approaches is labor intensive. It is the intension of this study to

*Andrew.Whittaker@cmr.uq.edu.au;

utilize quantitative structure-property relationships (QSPR)^{4,5} to develop a model for prediction of the refractive index of small molecules and polymers. A predictive model will allow candidate polymers to be assessed before they are synthesized, meaning that only those molecules with the desired properties need to be prepared. This has the result of accelerating the development cycle and also reducing costs.

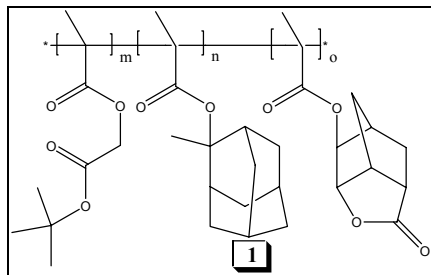


Figure 1: A typical example of a methacrylate based 'dry' 193 nm resist polymer.⁶

2. METHODOLOGY

2.1 QSPR

A diverse list of 126 compounds was chosen to develop the QSPR model. Refractive indices (at 589 nm and 293 K) were collected from chemical suppliers such as Sigma Aldrich.

The three-dimensional structures of the compounds were drawn using the AMPAC module in the CODDESSA software package. These structures were then optimized using the AM1 method.⁷ 791 descriptors were calculated for the 126 structures using the CODESSA software package and stored in the database for subsequent regression analysis. The descriptors were then screened for missing values, insignificance and high co-correlation. After the above procedure, 157 descriptors remained. A QSPR model was developed using a best multi-linear regression method.

2.2 Materials

Dicyclopentadiene, acrylic acid, tungstic acid, *t*-butanol, methacryloyl chloride, 2-methyl-2-adamantol, Aliquat 336, methacrylic acid, *t*-butyl chloroacetate, hydroxyethylmethacrylate, lithium chloride, sodium sulfide nonahydrate were obtained from Sigma Aldrich. Sulfur and sodium chloride was purchased from Asia Pacific Specialty Chemicals Ltd. Hydrogen peroxide was obtained from BDH.

2.3 Monomer Synthesis

Synthesis of bicyclo[2.2.1]hept-5-ene-2-carboxylic acid: Freshly cracked cyclopentadiene was added dropwise to an aqueous solution of acrylic acid and 5 M sodium chloride to yield 2-norbornene-*t*-5-carboxylic acid with a yield of 95%. The structure of the monomer was confirmed by ¹H and ¹³C NMR.

Synthesis of 2-hydroxy-4-oxatricyclo[4.2.1.0]nonan-5-one: A 30% aqueous solution of hydrogen peroxide was added dropwise to a mixture of 5-norbornene-2-carboxylic acid (10 mmol), tungstic acid (0.3 mmol) in *t*-butanol (15 mL). Following 48 hrs of reaction the solvent was reduced under reduced pressure to yield the hydroxyl lactone, which was recrystallized from hexane. The structure of the monomer was confirmed by ¹H and ¹³C NMR.

Synthesis of methacrylate 2: 2-hydroxy-4-oxatricyclo[4.2.1.0]nonan-5-one (37.5 mmol) and triethyl amine (45 mmol) were dissolved in anhydrous dichloromethane (100 mL). Methacryloyl chloride (45 mmol) was added dropwise to the mixture under a nitrogen atmosphere at 0 °C. Following addition the reaction was allowed to warm to room temperature and the reaction continued for 16 hours. The mixture was filtered and the filtrate was concentrated under reduced

pressure. The residue was diluted with ether and the organic phase was then washed with sodium carbonate (0.5 M) (*3 10 mL) followed by distilled water (*3 10mL). The crystalline residue was purified by recrystallization with hexane. The structure of the monomer was confirmed by ^1H and ^{13}C NMR.

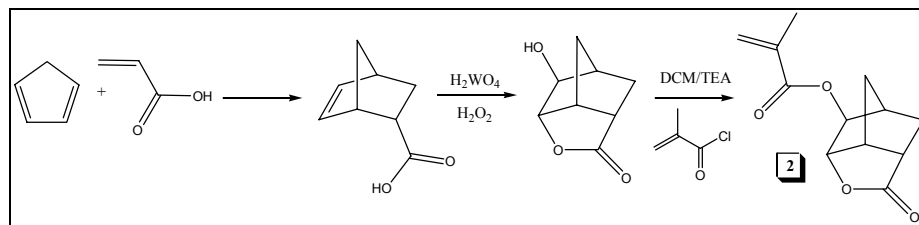


Figure 2: Synthesis of monomer 2

Synthesis of spaced ester 3: Potassium methacrylate (50.5 mmol), t-butyl chloroacetate (51 mmol) and a phase transfer catalyst (PTC), Aliquat 336 (0.01 mmol) were mixed with acetonitrile and refluxed (16 hrs). Following the reaction the acetonitrile solution was concentrated and the residue was diluted with ether (100 mL) and was washed with 0.5 M sodium carbonate (*3 10mL) and distilled water (*3 10 mL). The ether phase was concentrated to dryness and the residue vacuum distilled to yield a colorless oil. The structure of the monomer was confirmed by ^1H and ^{13}C NMR.

Synthesis of 2-methyl-2-admantyl methacrylate 4: 2-methyl 2-admantanol (31.8 mmol) and triethylamine (48.0 mmol) were mixed in dichloromethane ($\sim -20^\circ\text{C}$). Methacryloyl chloride (38.2 mmol) was added drop-wise into the cooled nitrogen purged solution. The reaction mixture was then stirred for 16 hours while maintaining the lowered temperature. The resultant mixture was filtered and the filtrate was washed with K_2CO_3 (10 mL *3) followed by distilled water (10 mL *3) and dried with anhydrous MgSO_4 . After evaporating the dichloromethane, the crude product was further purified by passing through a basic Al_2O_3 column using hexane/EtOAc as eluent. The final yield was 70%.

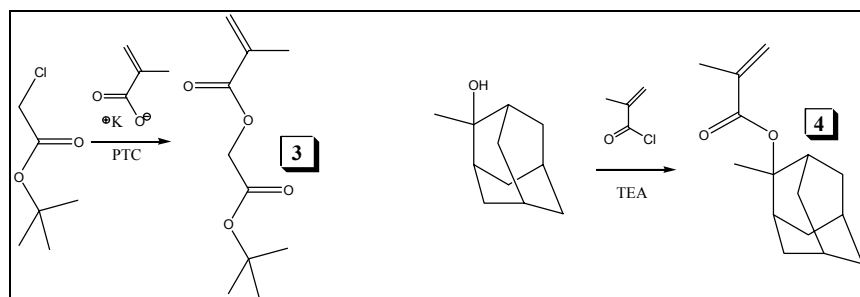


Figure 3: Synthesis of monomers 3 and 4

Synthesis of trithiomonomer 5: Freshly cracked cyclopentadiene (529 mmol) was added drop-wise into an aqueous solution of 5 M LiCl (20 mL) and 2-hydroxyethyl acrylate (327.6 mmol) at 0°C . The reaction mixture was allowed to warm to 25°C and was then stirred for 5 hours. The crude product was extracted with hexane to remove excess cyclopentadiene. The water phase was then extracted with EtOAc and dried. The yield of step 1 was almost quantitative. The step 1 product was dissolved in 200 ml of pyridine. Sulfur (0.99 mol) and $\text{Na}_2\text{S}\cdot 9\text{H}_2\text{O}$ (500 mg) were added to the solution. The solution was then heated to 110°C while being purged with N_2 for 16 hours. Following the reaction pyridine was evaporated and the crude product was purified through a neutral Al_2O_3 column. The yield of step 2 was 80%. The step 2 product (18 mmol) was reacted with methacryloyl chloride (21.6 mmol) and triethylamine (28 mmol) under the same conditions as described in the synthesis of monomer 4. The monomer 5 was obtained as a light yellow viscous liquid and the yield was 70%.

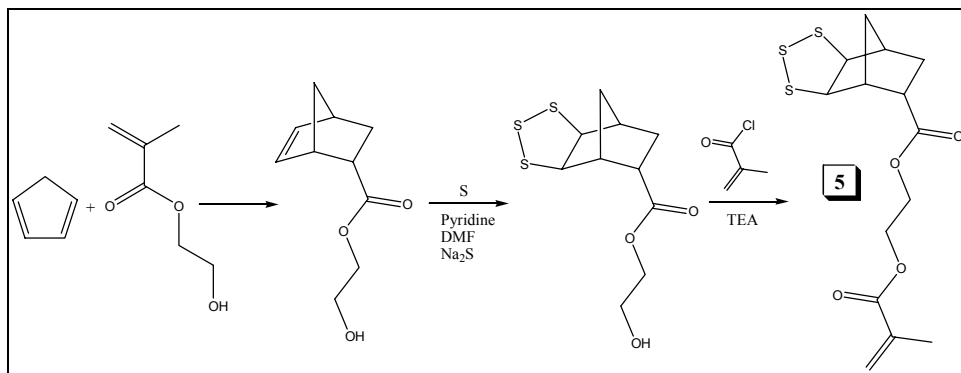


Figure 4: Synthesis of monomer 5

2.4 Polymer Synthesis

Polysulfones 6 and 7 were off the shelf polymers.

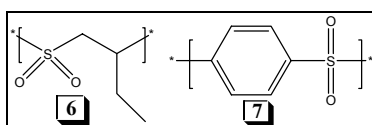


Figure 5: Structures of polymer 6 and 7

Polymerization to give Polymer 1: 60 mol% of monomer 2, 20 mol % monomer 3 and 20 mol% of monomer 4 were dissolved in THF with 1mol% AIBN. The vessel was sealed with a subaseal and degassed by purging with nitrogen for 5 minutes. The mixture was heated at 60 °C for 24 hours. The polymer was precipitated into methanol 3 times.

Polymerization to give Polymer 8: 60 mol% of thiomethyl ethyl methacrylate, 20 mol % monomer 3 and 20 mol% of monomer 4 were dissolved in THF with 1mol% AIBN. The vessel was sealed with a subaseal and degassed by purging with nitrogen for 5 minutes. The mixture was heated at 60 °C for 24 hours. The polymer was precipitated into methanol 3 times.

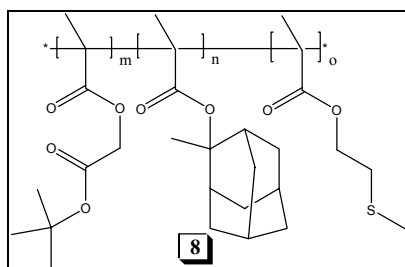


Figure 6: Structure of polymer 8 (m:n:o = 0.2 : 0.2 : 0.6)

Polymerization to give Polymer 9: 40 mol% of monomer 5, 60 mol % monomer 4 were dissolved in THF with 1mol% AIBN. The mixture was sealed with a subaseal and degassed by purging with nitrogen for 5 minutes. The mixture was heated at 60 °C for 48 hours. The polymer was precipitated into methanol 3 times.

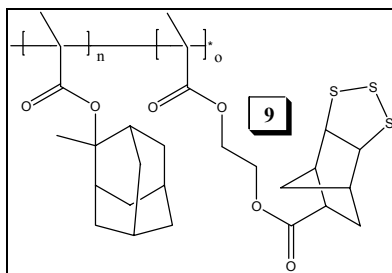


Figure 7: Structure of polymer 9 ($n : o = 0.6 : 0.4$)

2.5 Analysis

NMR: ^1H and ^{13}C NMR were performed on a Bruker 500MHz spectrometer with a TXI probe. For ^1H NMR at least 32 scans were acquired, for ^{13}C NMR at least 256 scans were acquired.

GPC: GPC was performed using a Waters 2690 module with THF as eluent.

3. RESULTS AND DISCUSSION

3.1 Development of a QSPR Model for Prediction of RI at 589 nm

Little is known about the refractive index of small molecules and polymers at 193 nm. Currently we are performing an on-going study of the RI of organic compounds at 193 nm, but at this point in time there is insufficient data to generate a quantitative model. Hence, we are using as a starting point the large volume of literature data available at 589 nm. At 589 nm, compounds with high RIs tend to contain easily-polarizable groups such as sulfur, aromatic groups and halogens. Katritzky and Ha have developed QSPR models for a number of polymers and organic compounds.^{4, 8} However, the compounds used to formulate the models were not particularly suited for this study, due to the lack of a diverse range high RI compounds including those with a range of sulfur-containing functionalities. Hence, we have compiled a diverse list of 126 compounds more suited for this study, to test the suitability of the literature models. The list includes molecules with a variety of sulfur functionalities as well as aromatics, halogens, esters, ethers, alkanes, and cyclics. When the models of Katritzky and Ha were applied to our list of compounds the fits of the models were unsatisfactory ($r^2 = 0.72$ and $r^2 = 0.22$ respectively). The main reason for this could be due to the increased number of sulfur-containing molecules that were selected for our model.

Due to the poor fit of previously published models for our set of compounds a new QSPR model was developed. The model obtained utilized 9 descriptors of the RI (Eq. (2)). The 9 descriptors were: heat of formation, translational entropy, minimum partial charge of a carbon atom, relative number of sulfur atoms, relative number of fluorine atoms, minimum bond order of a carbon atom, relative hydrogen donor charged surface area, polarizability and total enthalpy. The model is represented in Figure 8 where the experimental RI is plotted against the predicted RI. A high squared correlation coefficient of 0.96 was obtained with an error of $\pm 2\%$. However, it should be noted that one deficiency of the model was that it tended to under-predict the RI of some sulfur containing compounds.

$$RI = \sum_{i=1}^9 (k_i \cdot \text{Descriptor}_i) \quad (2)$$

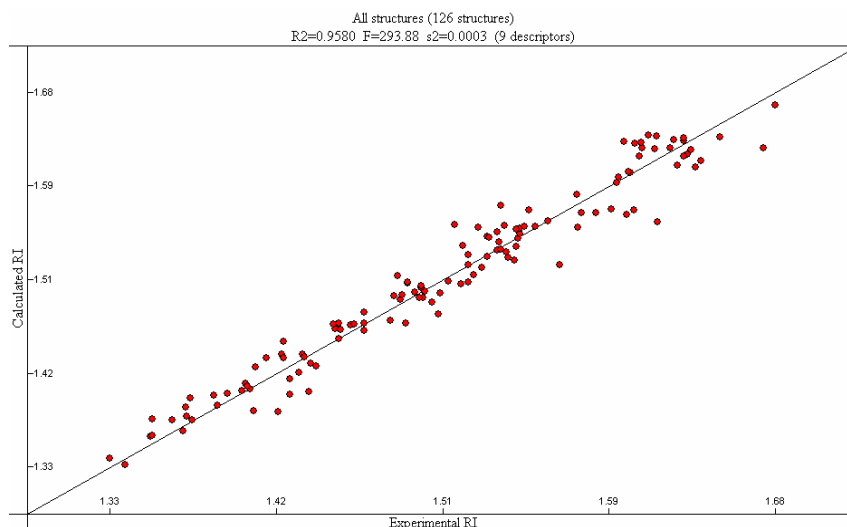


Figure 8 Linear plot of predicted versus experimental RI for the 9 parameter QSPR model.

3.2 Validation of the Model

The model was also validated using a 20 member external dataset, where the members of the validation set were not included in the establishment of the model. A linear plot of calculated RI versus experimental RIs is shown in Figure 9. This plot demonstrates that the predicted refractive indexes for the external dataset agree well with experimental values within $\pm 2\%$ error.

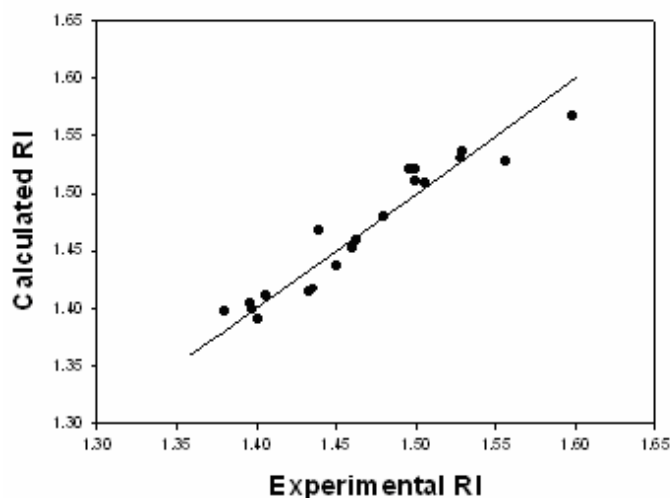


Figure 9 Calculated RI of external data vs. experimental values

3.3 Application of the Model to Polymers

It is expected that a high correlation between the RI of a linear polymer and the sum of contributions from its repeat units will be obtained because of the van Krevelen's group contribution theory⁹. Of course, polymer configuration will have some impact on refractive index, but it is anticipated that this will be a minor contribution for random amorphous polymers, which are main focus of this study. Fig. 10 shows the correlation for some typical polymers and their corresponding repeat units (modeled as hydrogenated monomer). The squared correlation coefficient obtained was good ($R^2 = 0.90$, $RI_{\text{polymer}} = RI_{\text{monomer}} + 0.09$), although this is somewhat lower than the original model. We hypothesize that the difference between RI_{polymer} and RI_{monomer} is due to the change in density (Δd) that occurs during polymerisation. The difference in Δd during polymerization for different monomers could be a cause for the increased scatter in Figure 10.

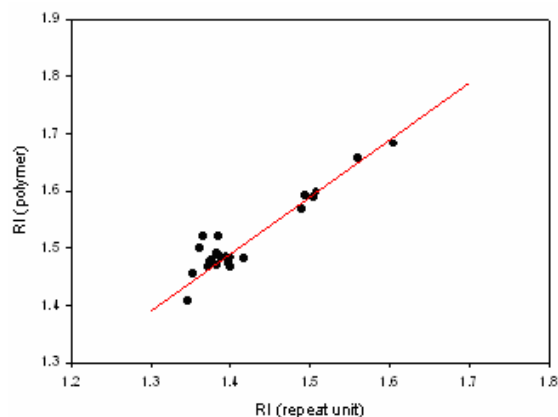


Figure 10: Correlation of RI of polymers with that calculated from the contributions from their repeat units

3.4 Extrapolation of the Model to 193 nm

It is also necessary to confirm that there is correlation between the refractive index at 589 nm and 193 nm. The well-known Cauchy equation (Eq (3)) describes the refractive index dispersion absorption is not significant. Fig. 11 shows the refractive index dispersion of some common compounds. The curves shown can be fitted with the Cauchy equation, which indicates that if the refractive index of a compound is high at 589 nm, it will also be high at 193 nm, providing the compound is non-absorbing. From the above analysis, we should be able to use the QSPR predictions at 589 nm as a starting point to develop new resist polymers with high refractive index at 193 nm.

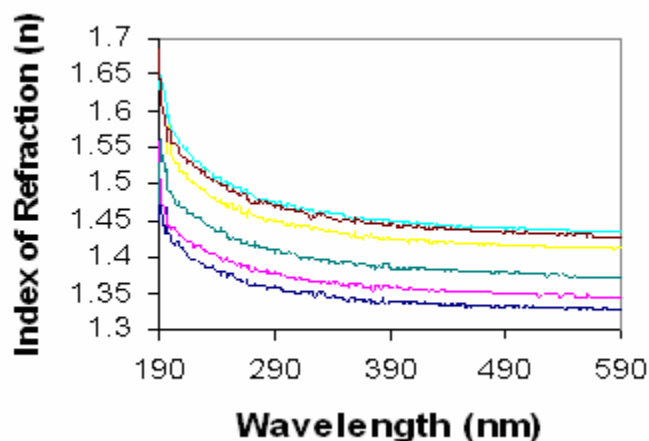


Figure 11: Refractive index dispersion (from top to bottom: butyrolacetone, cyclohexane, THF, ethyl acetate, acetonitrile, HPLC water)

$$n = B_0 + \frac{B_1}{\lambda^2} + \frac{B_2}{\lambda^4} + \dots \quad (3)$$

Table 1 lists the predicted RIs at 589 nm and the experimental values of RI at 589 nm. In general, the QSPR model was able to predict the RI of the polymers at 589 nm, although polymer **9** was slightly under predicted (the model was known to under predict some sulfur functionalities, see 3.1) and surprisingly significantly over predicted the standard ArF polymer **1**. A possible reason for the over prediction of polymer **1** is that the polymer has a higher proportion of bulky side groups and it is anticipated that this will produce a less dense polymer and hence a lower refractive index. Future models may need to take this variable into consideration.

Table 1: Values of RI for synthesized polymers.

Polymer	Predicted RI at 589 nm	Experimental RI at 589
1 (Std ArF resist Polymer)	1.57	1.51
6 (poly-1-butene sulfone)	1.54	1.54
7 (polyphenylene sulfone)	1.61	1.62
8	1.55	1.54
9	1.63	1.59

3.5 RI of Polymers at 193 nm

Figure 12 (left) shows the wavelength dependence of the standard ArF polymer (**1**) and the two polysulfones (**6** and **7**). The standard ArF polymer has a RI of 1.7 at 193 nm. Polysulfone **6** shows an increased RI of 1.76, which indicates that inclusion of the sulfone group has a positive effect on RI. However, **7** has a RI of ~1.51, which is significantly lower than the standard polymer (**1**). This was not predicted by the QSPR model. The reason for this is that the Cauchy equation fails to describe the RI of the polymer below 310 nm. This drop in RI is due to the high absorbance of the polymer at 193 nm indicating that aromatic compounds will be unsuitable due to their high absorbance.

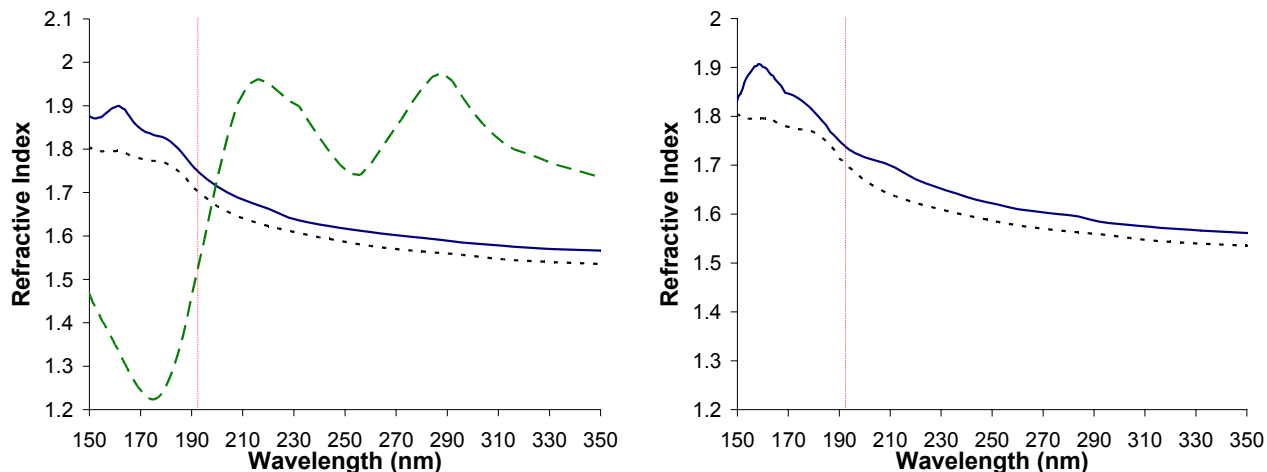


Figure 12: (left) Wavelength dependence of RI of the standard resist polymer **1** (small dash), poly(1-butene sulfone) **6** (solid) and polyphenylene sulfone **7** (long dash). (Right) standard ArF polymer **1** (short dash) and polymer **8** (solid)

Fig. 13 compares the experimental refractive index values of polymer **9** with the standard polymer **1**. The RI of polymer **9** was 1.88 at 193 nm, which is significantly higher than the standard ArF polymer **1**. Currently we are in the process of imaging this polymer using 193 nm immersion tools.

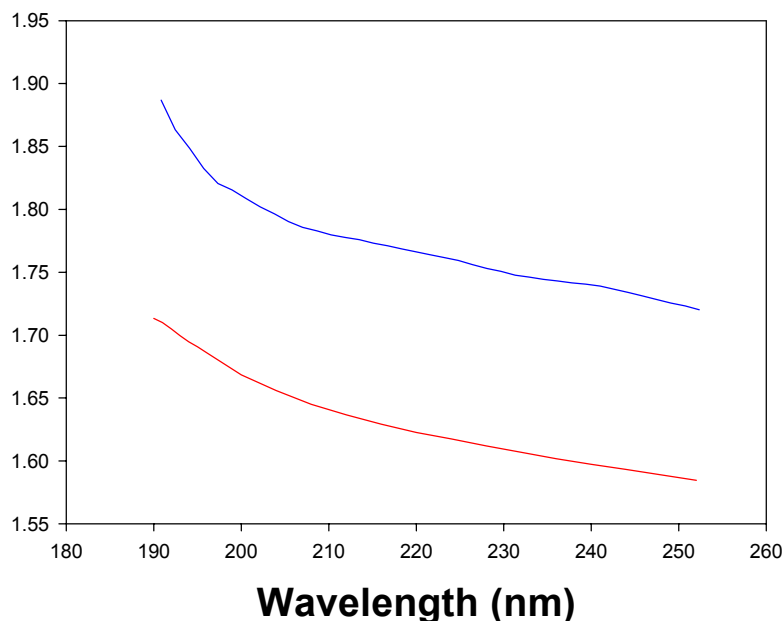


Figure 13: Wavelength dependent of the RI of polymer 9 (top) in comparison with the standard polymer 1 (bottom)

4. CONCLUSIONS

A QSPR model was developed that could accurately predict the RI of organic compounds at 589 nm. The model was also adapted to predict the RI of polymers at 589 nm. However, the accuracy of this adaptation was slightly less than the original model. Polymers have been synthesized with RIs between 1.76 and 1.88, values which are significantly higher than standard ArF polymers which have RIs of approximately 1.7 at 193 nm. The QSPR model was not entirely accurate when extrapolated to 193 nm. This was due in part to the failure of the Cauchy equation to fit the RI dispersion of some polymers, in particular aromatic-containing polymers. With sufficient data at 193 nm it is anticipated that a model with similar accuracy to the 589 nm model will be developed. RI measurements of organic compounds at 193 nm are currently being performed to develop a QSPR model at that wavelength.

ACKNOWLEDGEMENTS

SEMATECH for project funding, Queensland State Government for funding of Smart State Fellowship for IB, Danny Miller from SEMATECH and Chris Taylor from University of Texas for RI measurements of the polymers, Mike Whittaker for running GPC of polymers.

REFERENCES

- ¹ Conley, W. and Mack, C., Intl. Symp. Immersion and 157 nm Lithography Vancouver 2004
- ² Khojastch, M., Chen, K. R., Kwong, R., Lawson, M., Varanasi, P. R., Patel, K. SPIE, 5039, 187 (2003)
- ³ Blakey, I. Conley, W. George, G.A.Hill, D. Liu, H. Whittaker, A.K. Zimmerman P., Intl. Symp. Immersion and 157 nm Lithography Vancouver 2004
- ⁴ Alan R. Katritzky, Sulev Sild, and Mati Karelson, *J. Chem. Inf. Comput. Sci.* **1998**, *38*, 840-844
- ⁵ Alan R. Katritzky, Sulev Sild, and Mati Karelson *J. Chem. Inf. Comput. Sci.* **1998**, *38*, 1171-1176
- ⁶ Khojastch, M., Chen, K. R., Kwong, R., Lawson, M., Varanasi, P. R., Patel, K. SPIE, 5039, 187 (2003)
- ⁷ Dewar, M. J. S.; Zoebisch, E. G.; Healy, E. F.; Stewart, J. J. P. *J Am Chem Soc* 1985, *107*, 3902
- ⁸ Ha, Zhanyao; Ring, Zbigniew; Liu, Shijie, *Energy & Fuels* **2005**, *19*, 152-163
- ⁹ Van Krevelen, D. W., "Properties of polymers : their correlation with chemical structure; their numerical estimation and prediction from additive group contributions" Elsevier, Amsterdam, 1990. 3rd Ed.